Immobilization of laccase onto a porous nanocomposite: application for textile dye degradation — Source link

Sedef Ilk, Deniz Demircan, Semran Sağlam, Necdet Sağlam ...+1 more authors

Related papers:

- Enhancing catalytic performance of laccase via immobilization on chitosan/CeO2 microspheres.

- Laccase-conjugated thiolated chitosan-Fe3O4 hybrid composite for biocatalytic degradation of organic dyes

- Preparation of Laccase Immobilized Cryogels and Usage for Decolorization

- The Biocatalytic Degradation of Organic Dyes Using Laccase Immobilized Magnetic Nanoparticles

- A novel method for improving laccase activity by immobilization onto copper ferrite nanoparticles for lignin degradation.

Share this paper:

View more about this paper here: https://typeset.io/papers/immobilization-of-laccase-onto-a-porous-nanocomposite-38jhgem1rz

Immobilization of laccase onto a porous nanocomposite: application for textile dye degradation

Sedef İLK[1,*], Deniz DEMİRCAN[2], Semran SAĞLAM[3], Necdet SAĞLAM[4], Zakir M. O. RZAYEV[4]

[1]Ayhan Şahenk Faculty of Agricultural Sciences and Technologies, Niğde University, Niğde, Turkey
[2]Department of Chemistry, Faculty of Science, Hacettepe University, Ankara, Turkey
[3]Department of Physics, Faculty of Sciences, Gazi University, Ankara, Turkey
[4]Department of Nanotechnology and Nanomedicine, The Institute of Science and Engineering,
Hacettepe University, Ankara, Turkey

Abstract: Poly(MA-*alt*-MVE)-*g*-PLA/ODA-MMT nanocomposite was prepared by self-catalytic interlamellar graft copolymerization of L-lactic acid (LA) onto poly(maleic anhydride-*alt*-methyl vinyl ether) copolymer in the presence of octadecyl amine-montmorillonite (ODA-MMT) organoclay. FTIR, ^{1}H (^{13}C) NMR, XRD, and SEM-TEM were utilized for characterizing the resultant nanocomposite. Laccase from *Trametes versicolor* was immobilized onto the prepared nanocomposite by adsorption or covalent coupling. Decolorization of Reactive Red 3 from aqueous solution by laccase immobilized on the nanocomposite was studied in different conditions (pH, temperature, dye concentration, and reaction time) to investigate the decolorization activity with repeated use and storage. The results indicated that more than 77% of the activity of laccase immobilized systems was retained at the end of 10 cycles. The final decolorization capacity of the immobilized laccase was significantly higher (65%) than that of free laccase (33%) in the chosen optimized conditions (pH 5, 20 °C, 0.05 mg/mL laccase concentration, and 90 min).

Key words: Nanocomposite, functional copolymer, interlamellar graft copolymerization, enzyme laccase, immobilization, reactive dyes, decolorization

1. Introduction

Synthetic dyes are commonly used in the textile, paper, printing, cosmetics, and pharmaceutical industries to give a permanent color to materials.[1] The widespread and increasing use of reactive dyes polyaromatic molecules is a major problem if discharged into environment without any treatment. Color can be removed from wastewater by chemical and physical methods such as adsorption, electrochemical, ion-exchange, and oxidation methods.[2] Although there are different options, enzymatic oxidation of the dye using fungal oxidoreductases such as laccases has received great attention in recent years due to efficient decolorization of the effluent.[3,4] Laccases have been applied in several industrial areas including decolorization of textile dyes, biobleaching, biosensing, bioremediation, chemical synthesis, and wine stabilization owing to their ability to oxidize phenolic compounds and their promising biocatalyst properties.[5] Despite the unique catalyst properties of laccase, the enzyme is rapidly inactivated when it comes to applications due to environmental effects. Furthermore, it is

*Correspondence: sedefilk@nigde.edu.tr

difficult to reuse due to separation from the reaction system.[6] Owing to their improved stability and storage ability, the immobilization of enzymes offers several advanced applications such as the system of enzyme is easier to operate, the enzyme can be reused, and the cost of the process reduced.[7] The reusability and the cost of immobilized enzymes constitute a great advantage over free enzymes.[8] In an immobilization study, the most crucial point is to immobilize a bioactive reagent onto a support bearing a functional group on the surface. The surface functionalized supports with reactive groups increase the loading capacity and stability of the protein immobilization.[9] Generally, natural and synthetic polymers are used for the functionalization of support.[10]

Poly(MA-*alt*-MVE), being a matrix polymer, has been employed for immobilization of proteins, peptides, and saccharides[11,12] as well as for protein adsorption from flowing solutions.[13] Recently, MA grafted thermoplastic polymers[14,15] and PLA-*g*-MA[16,17] were studied as effective polymer compatibilizers for various reactive polymer blends and their nanocomposites by many industrial and academic researchers. Kontou et al.[18] investigated the effects of two different types of nanofillers (silica and MMT) at three different weight fractions as well as their mixtures on the thermomechanical properties of PLA. It is well known that the decolorization efficiency of laccase enzyme and its immobilized derivatives essentially depends on many factors such as (1) the structure of membrane for which the synthesis is available by both chemical and physical interactions, (2) the origin and structure of utilized polymer systems, (3) the concentration of enzyme or immobilized enzyme, (4) temperature, (5) pH of the medium, and (6) immobilization period. Therefore, the evaluation of the effects of these parameters on decolorizing and their optimization are very important. The goals of the present study were to develop a novel approach for the design and synthesis of functional copolymer-*g*-PLA layered silicate nanocomposite in the presence of organo-MMT clay (octadecyl amine-MMT) as catalyst-nanofiller (3.2 wt %); to immobilize laccase from *Trametes versicolor*, which is used in the decolorization of industrial reactive dyes, on this synthesized nanohybrid structure under different conditions such as laccase concentration, reaction time, pH, and temperature; and to measure decolorization activity of the laccase enzyme immobilized systems at different Reactive Red 3 dye concentration, reaction time, pH, and temperature conditions. For this purpose, poly(MA-*alt*-MVE)-*g*-PLA/ODA-MMT nanocomposite was synthesized by self-catalytic interlamellar graft copolymerization of L-lactic acid (LA) onto poly(maleic anhydride-*alt*-methyl vinyl ether) in the presence of octadecyl amine-montmorillonite (ODA-MMT) organoclay. The chemical and physical structures and morphology of the intercalated nanocomposite were characterized by FTIR, ^{1}H (^{13}C) NMR, XRD, SEM, and TEM. Laccase enzyme was immobilized on the fabricated nanocomposite either by adsorption or by covalent binding. Finally, the decolorization of Reactive Red 3 by laccase immobilized nanostructure was studied. The stability and activity of decolorization of the laccase immobilized systems were investigated at different pH values, temperatures, initial dye concentrations, and reaction times.

2. Results and discussion

2.1. Properties of poly(MA-*alt*-MVE)-*g*-PLA nanocomposite

We employed a facile synthesis of poly(MA-*alt*-MVE)-*g*-PLA graft copolymer silicate layered nanocomposite by self-catalysis in situ processing in the presence of ODA-MMT clay (3.2 wt%) at a relatively low temperature (30–40 °C) without the need for a hazardous tin-containing catalyst, a vacuum system, or a high reaction temperature (120 °C). It was shown that ODA-MMT clay, with a dual functionality, serves both as a nanofiller (layered silicate) and a catalyst component in the formation of LA grafted copolymer complex. The synthetic pathways of the nanocomposite are represented in Figure 1.
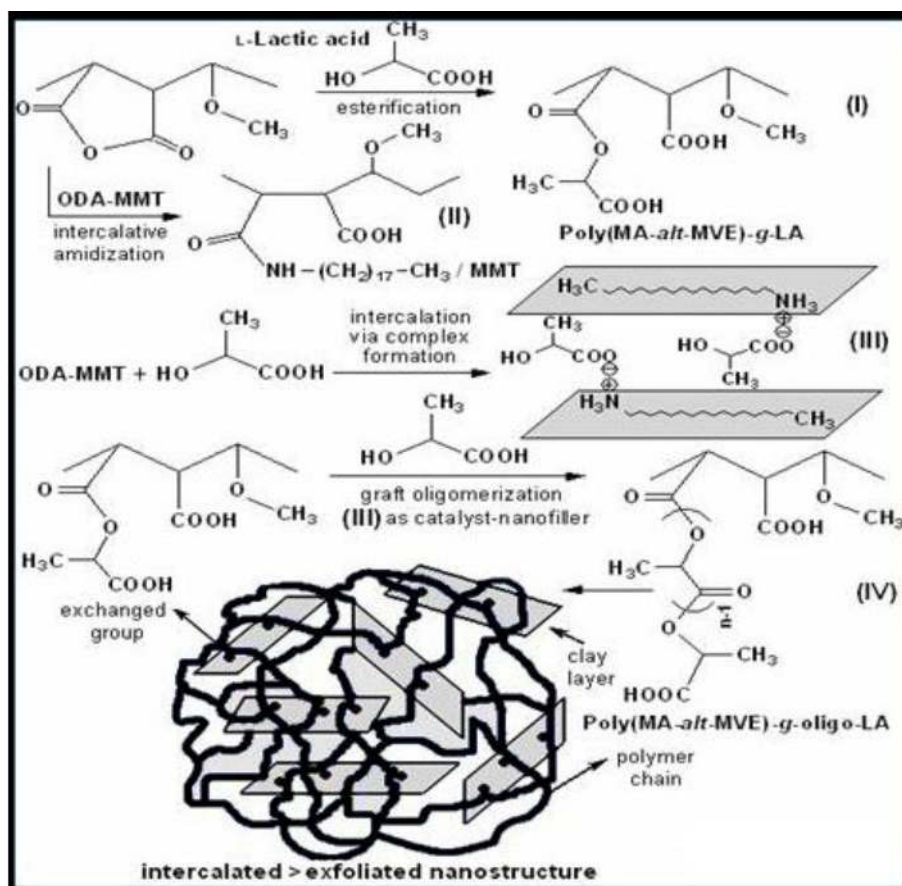
Figure 1. Schematic representation of synthetic pathways for preparation of poly(MA-*alt*-MVE)-*g*-PLA/ODA-MMT nanocomposites via interlamellar graft copolymerization of lactic acid monomer onto copolymer in the presence of pre-intercalated LA-ODA-MMT complex as a catalyst-nanofiller.

The chemical structure of the synthesized poly(MA-*alt*-MVE)-*g*-PLA/ODA-MMT organoclay composite was confirmed by FTIR (Figure 2) and ^{1}H and ^{13}C NMR spectroscopy (Figure 3).
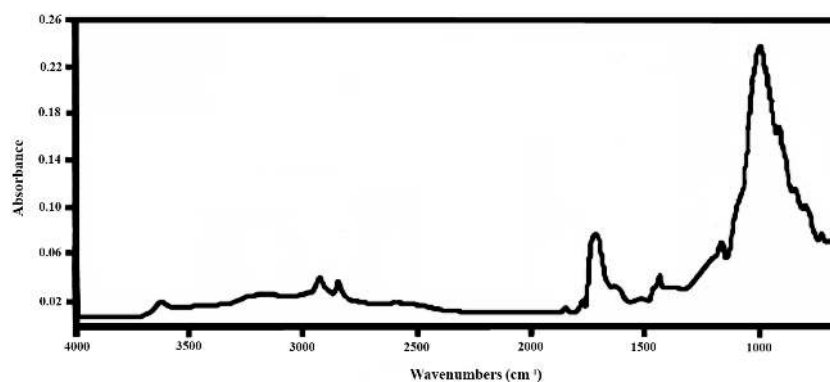
Figure 2. FTIR spectra (KBr pellet) of poly(MA-*alt*-MVE/ODA-MMT nanocomposite synthesized by interlamellar graft copolymerization in PLA solution.
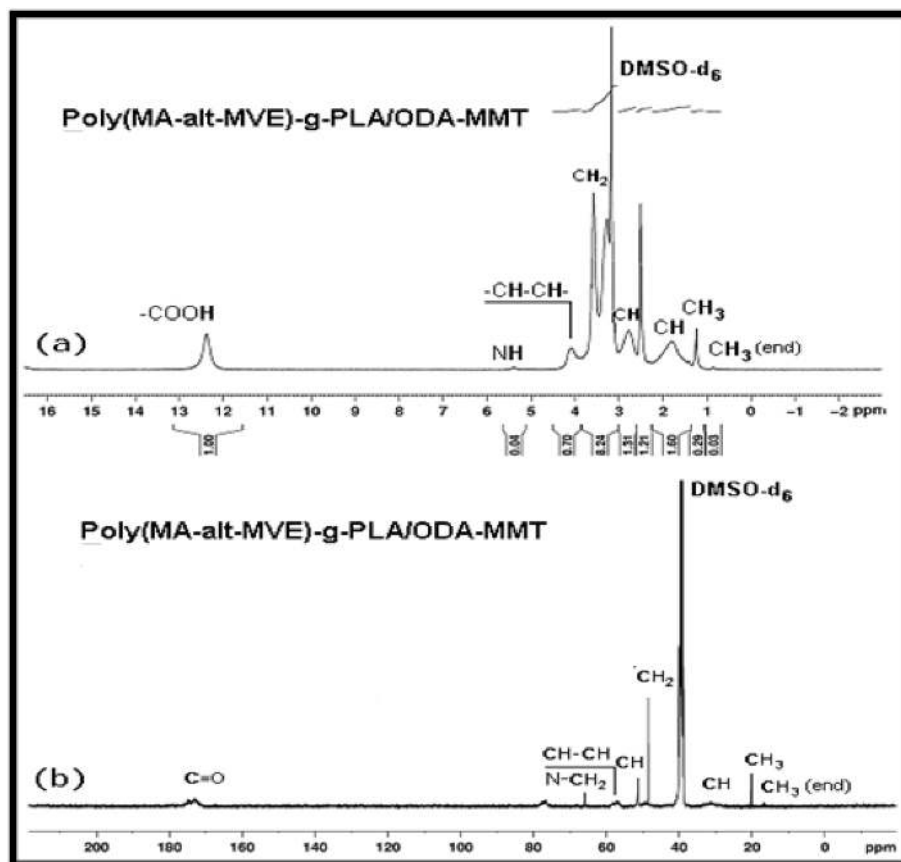
Figure 3. (A) ^{1}H and (B) ^{13}C NMR spectra of poly(MA-*alt*-MVE) ($M_n = 80,000$ Da)-g-PLA/ODA-MMT nanocomposite in DMSO-d$_6$.

As shown in Figure 2, a band appears at 1510 cm^{-1} with a symmetric stretching vibration via H-bonding of the –COO$^-$ group. The formation of a new characteristic band at 1640 cm^{-1}, corresponding to the carboxylic groups in –NH$_3^+$.$^-$OOC– complexes indicates chemical and physical interactions between functional copolymer chains and organic modified silicate layers. The existence of a strong band at 1190 cm^{-1} and a band at 1376 cm^{-1} from CH$_3$ groups of branched PLA indicate the formation of graft copolymer fragments in the nanocomposite.

Similar chemical shifts were displayed in the ^{1}H and ^{13}C NMR spectra of the copolymer-g-PLA silicate layered nanocomposite (Figures 3A and 3B). In the spectra, the characteristic chemical shifts related to CH (2.65 ppm) and CH (46.12 ppm), –COOH (12.35 ppm), C=O (162 ppm), C=O (165 ppm), and CH$_3$ (19.95 ppm) groups from branched PLA were also observed.

The physical structure of the nanosystems was investigated by XRD analysis. The XRD pattern of the poly(MA-*alt*-MVE)-g-PLA/ODA-MMT nanocomposite is illustrated in Figure 4. The nanohybrid prepared in LA solution by interlamellar graft copolymerization shows an amorphous structure because the branched PLA chains play the role of an internal plasticizing agent in the nanocomposite structure. The results of XRD analysis indicated that the copolymer-g-biopolymer/clay nanosystems synthesized by interlamellar graft copolymerization predominantly exhibit a semicrystalline structure and better intercalation/exfoliation of PLA grafted copolymer chains between silicate galleries.
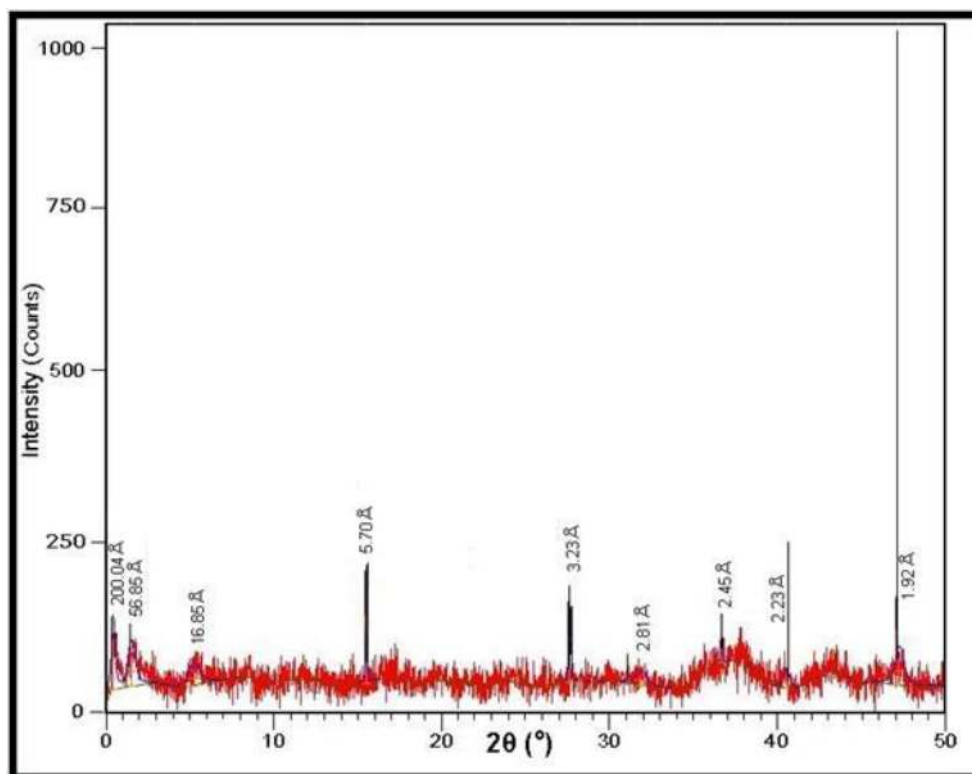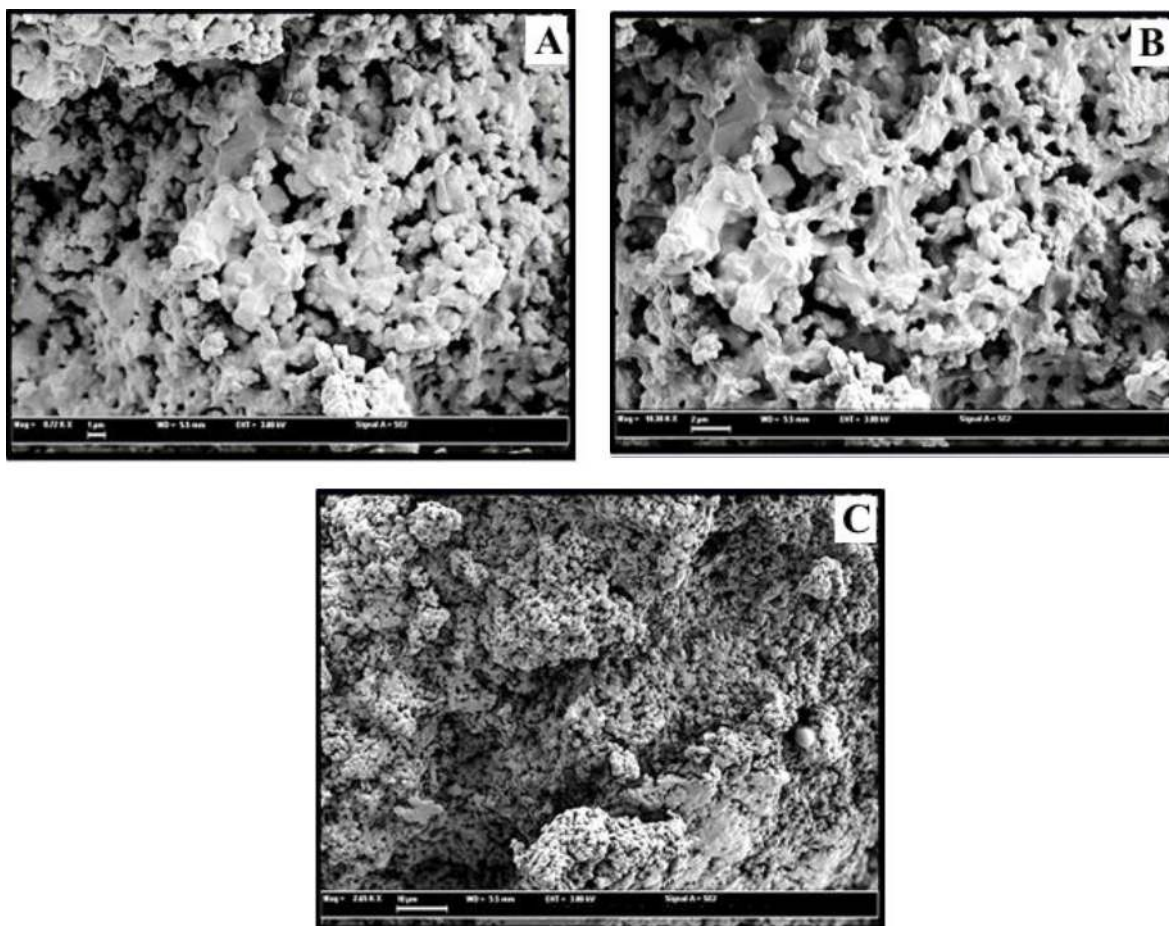
Figure 4. XRD patterns of poly(MA-*alt*-MVE)-*g*-PLA/ODA-MMT nanocomposite prepared with M_n 80,000 Da of a matrix copolymer.

It is well known that SEM indicates surface morphology–structure–property relationships of polymer composite and polymer/organo-silicate nanocomposite on various length scales. The results of SEM analysis (Figures 5A–5C) very clearly display the finely dispersed surface morphology of the copolymer-g-PLA/organoclay nanocomposite. In agreement with these images, the nanocomposite exhibits micro- and nanoporous morphologies due to the elimination of water and/or LA-monomer traces from clay layers after their in situ delamination.

The results of TEM analysis are illustrated in Figure 6. The presence of single and partially agglomerated clay layers dispersed in the graft copolymer matrix, which is prepared by the use of an alternating copolymer with relatively low molecular weight (M_n 80,000 Da), displays the formation of dispersion of delaminated and encapsulated clay platelets with predominantly intercalated nanostructures (Figure 6).

The internal morphology of the nanocomposite also depends on the concentration of alternating copolymer in the reaction mixture. Agreeing with TEM images (Figures 6A–6F), a decrease in copolymer concentration from 0.16 to 0.08 g/mL results in a gradual transformation of the asymmetric morphology images to the self-assembled nanocore-shell morphology. A relatively homogeneous phase distribution with core-shell morphology was observed for nanocomposites prepared in the presence of a low molecular weight alternating copolymer at a lower concentration in the reaction mixture (Figure 6F). The formation of core-shell morphology in this nanosystem, which usually is not observed for polymer layered silicate nanocomposites, can be explained by its tendency to form self-assemble nanostructures through specific physical and chemical interfacial interactions. Thus, TEM observations indicate that the morphologies changed from asymmetric to core-shell type of intercalated/exfoliated structures that occur between silicate galleries. The structure of individual dispersion

266

Figure 5. SEM micrographs of poly(MA-*alt*-MVE)-*g*-PLA/ODA-MMT composite prepared with a matrix copolymer (M_n = 80,000 Da) in LA solution. Scale of images: A: 1 μm $\times$ 8000, B: 2 μm $\times$ 10,000 and C: 10 μm $\times$ 20,000 magnification.

of delaminated clay platelets and therefore an exfoliated nanostructure depend on the presence of clay layers dispersed in the copolymer matrix. In the presence of the ODA-MMT clay, a relatively homogeneous phase is observed that is reasonably in agreement with the SEM results.

2.2. Immobilization of laccase onto poly(MA-*alt*-MVE)-*g*-PLA/ODA-MMT nanocomposite

Laccase was immobilized onto the poly(MA-*alt*-MVE)-*g*-PLA/ODA-MMT nanocomposite by physical and chemical (covalent bonding in the presence of EDAC catalyst) adsorption. To determine the immobilized amount of laccase on the poly(MA-*alt*-MVE)-*g*-PLA/ODA-MMT nanocomposite, the reaction mixtures of immobilized laccase and support suspensions were separated. Laccase concentrations before and after immobilization were determined spectrophotometrically at 280 nm and Bradford's method was used to determine the total protein content. Therefore, it can be estimated that the immobilized amounts of laccase on the poly(MA-*alt*-MVE)-*g*-PLA/ODA-MMT nanocomposite can reach about 500 mg g nanocomposite^{-1} by physical adsorption and 328 mg g nanocomposite^{-1} by covalent attachment. Physical adsorption gave a 34.5% higher binding result compared to covalent binding. Before laccase immobilization, the groups (–COH) of the EDAC molecule were possibly covalently attached to the amino groups on the surface of the nanocomposites, which decreases
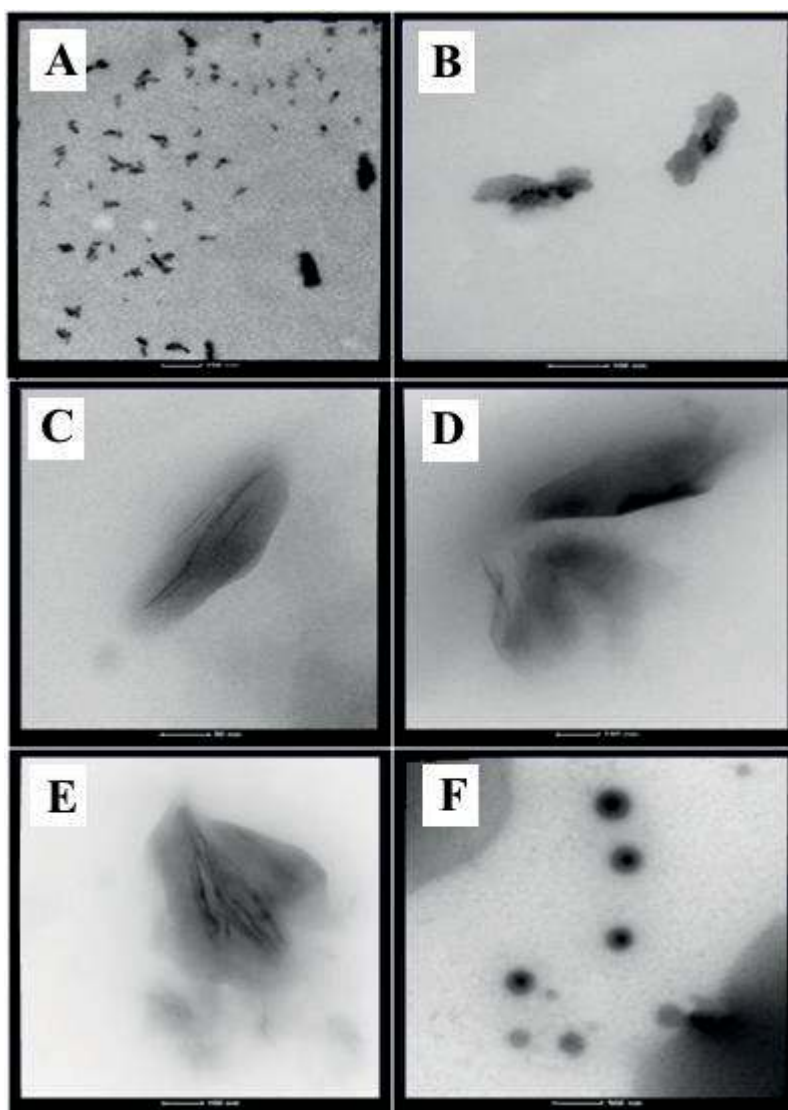
Figure 6. TEM images of poly(MA-*alt*-MVE)-*g*-PLA–ODA-MMT (3.2% wt) nanocomposite prepared with $M_n =$ 80,000 Da of matrix copolymer in LA solution: (A: 500 nm and B:100 nm) 0.16 g/mL, (C and D: 100 nm) 0.1 g/mL, and (E: 100 nm and F: 500 nm) 0.08 g/mL.

the amount of functional groups reacting with laccase molecules. Owing to the decreased pore size causing hindered diffusion effects may be obtain such slow immobilized performance of covalent binding.[19,20] Physical immobilization methods disturb the enzyme much less than covalent immobilization because the covalent bonds can confuse the enzyme's native structure; consequently covalent immobilizations reduce the enzyme activity.[21,22] As a result of the immobilization behavior of laccase on the support, physical adsorption was chosen to perform the rest of the experiment.

2.3. Activity assay of the immobilized laccase

The activity of the free and immobilized laccase was measured as explained in the Experimental section. The immobilized enzyme showed lower activity (3.86 U/mg) values than the free enzyme (5.56 U/mg) (data not

shown) for the oxidation of the soluble substrate (ABTS). These data indicate that the immobilized laccase is not denatured; substrate can easily diffuse into the porous channels of supports and it can be oxidized by the immobilized laccase.[19,23]

The optimization parameters of the immobilization of laccase onto the nanocomposite were studied. Figure 7A shows the immobilized amounts of laccase on the supports with different (0.01–0.15 mg/mL) laccase concentrations. The immobilized amount of laccase increases up to a certain laccase concentration (0.05 mg/mL) and above this concentration no more laccase can be immobilized. The optimum laccase concentration was determined as 0.05 mg/mL.[24] Figure 7B shows the immobilized amounts of laccase on the supports as a function of time when the laccase concentration is 0.05 mg/mL. The immobilization of laccase on the poly(MA-*alt*-MVE)-*g*-PLA/ODA-MMT nanocomposite is fast, and equilibrium adsorption can be achieved in 60 min.
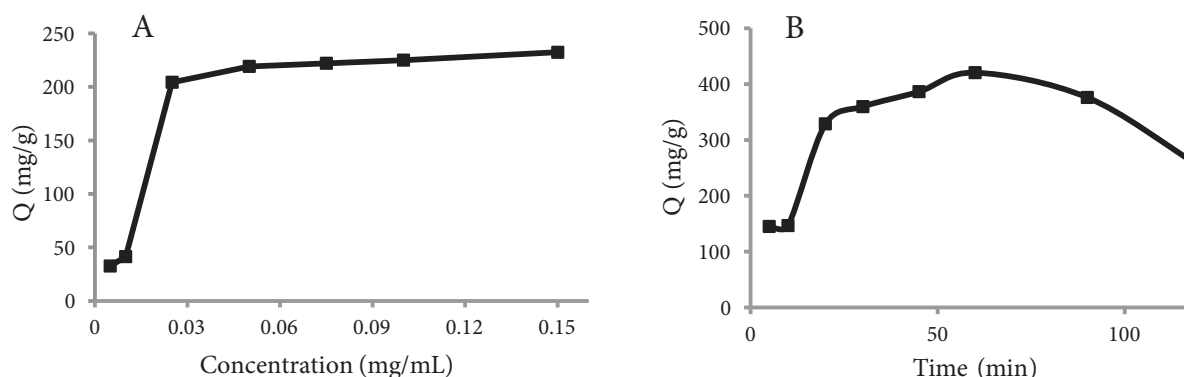

Figure 7. (A) Immobilized amounts of laccase on the supports as a function of laccase concentration. (B) Immobilized amounts of laccase on the supports as a function of time.

Important parameters such as pH and temperature should be controlled during adsorption of enzyme to obtain reproducible results since these parameters influence the stability and conformational structure of proteins. Figure 8A shows the amount of enzyme adsorbed onto the poly(MA-*alt*-MVE)-*g*-PLA/ODA-MMT nanocomposite at different pH values. In our study, the maximum laccase adsorption value was obtained at pH 4.5. Significantly, a lower laccase adsorption was obtained for the nanocomposite in all other tested pH regions. Laccase immobilization efficiency decreased sharply in highly acidic (lower than 3.5) or alkaline conditions (higher than 5.5) probably due to the decreased binding sites between nanocomposites and enzyme laccase.[25,26]

Figure 8B shows the effect of temperature on the absorption of laccase on the nanocomposite. The optimum activity was obtained in the temperature range 30–40 °C and the increase in temperature was followed by a stepwise decrease in activity. In addition, immobilization resulted in a slight broadening of the curve at this temperature, in agreement with other investigations.[27]

2.4. Decolorization of dye using free and immobilized laccase

The results of the investigations related to the effects of different parameters on decolorization of azo-dye with free enzyme and immobilized enzyme are illustrated in Figures 9A and 9B and 10A and 10B.
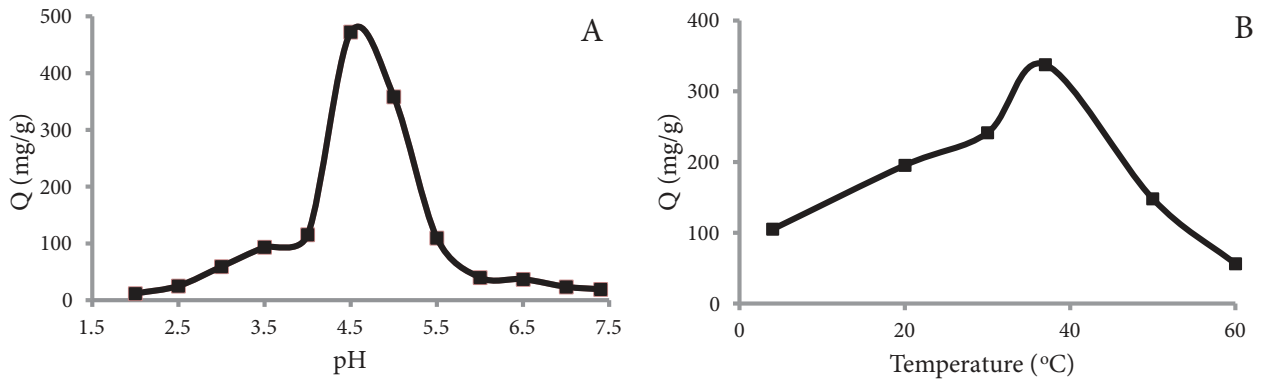
Figure 8. (A) Adsorption activity of the immobilized laccase at different pH values. (B) Effect of temperature on the adsorption activity of the immobilized laccase.
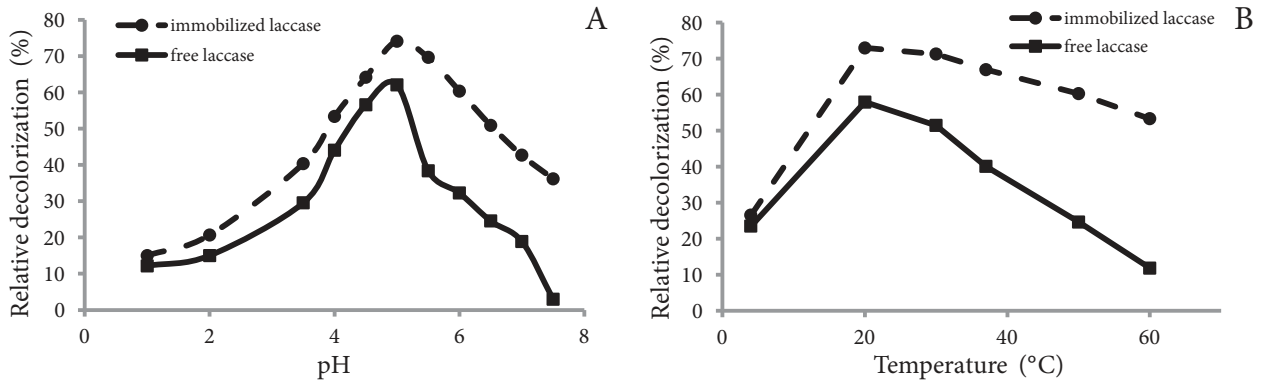
Figure 9. Effects of (A) pH medium and (B) temperature on the decolorization of Reactive Red 3 dye by pristine laccase enzyme and immobilized laccase enzyme.
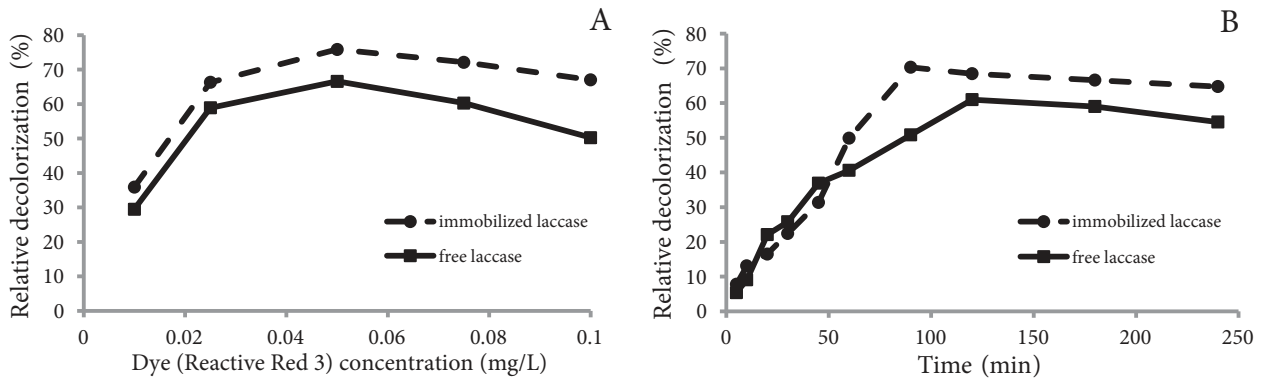
Figure 10. Effects of (A) concentration of azo-dye and (B) contact time on the decolorization of Reactive Red 3 dye by pristine laccase enzyme and immobilized laccase enzyme.

2.4.1. Influence of pH and temperature on decolorization

A higher adsorption capacity of laccase onto copolymer layered silicate matrix and significant decolorization of the tested azo-dye by the free and immobilized laccase were observed in acidic medium (pH 5) at 20 °C

(Figure 9A). The majority of the fungal laccases optimally act in acidic pH.[28] The relative decolorization of free laccase at optimum pH (pH 5) was 62%, while decolorization in the case of immobilized laccase at optimum pH (pH 5) was 74%.[29] In comparison with the free laccase, the immobilized laccase exhibited more than 60% of the maximum decolorization activity with a wider pH range between 4.5 and 6. While free laccase presented a decrease of 60.2% in the activity under more alkaline conditions such as pH 7.5, the activity of immobilized laccase decreased 38.6%. These results showed that free laccase was more sensitive to the alkaline environment than immobilized laccase because of the effect of the charge of the carrier.[30,31]

The highest decolorization percentage in the case of synthetic dye was obtained at the optimum temperature (20–30 °C) (Figure 9B). At the elevated temperature of 60 °C, relative decolorization of dye by free laccase decreased below 15%. However, in the case of immobilized laccase above 50% of initial decolorization remained at 60 °C. In comparison with the free laccase, the immobilized laccase resulted in a broader profile, the relative activity being maintained at over 50% within the temperature range 20–60 °C. The increase in optimum temperature was caused by the changing physical and chemical properties of the enzyme. The physical adsorption via amino groups of the immobilized laccase may result in higher activation energy for the molecule to reorganize the proper conformation for the binding to substrate.[32]

2.4.2. Effect of dye concentration and time function on laccase-mediated decolorization

Figure 10A shows the decolorization rate of the Reactive Red 3 dye by free and immobilized laccase onto supports as a function of dye concentration. It can be observed that the decolorization rate of dye by the immobilized and free laccase increases with the increase in dye concentration up to 0.05 mg/L. Above this dye concentration, the decolorization activity of the immobilized laccase decreased slowly compared to the free laccase.

The decolorization rate of Reactive Red 3 by free and immobilized laccase on the poly(MA-*alt*-MVE)-*g*-PLA nanocomposite as a function of time is illustrated in Figure 10B. The degradation of the Reactive Red 3 by immobilized laccase increased rapidly in 90 min (decolorization rate 71%) as a function of time, while the optimum time for decolorization of free laccase was between 120 and 180 min (decolorization rate 59%). These results indicated that decolorization by immobilized enzyme is faster than for free laccase.

2.5. Storage stability and reusability

The free and the laccase immobilized on the spacer-arm attached nanocomposites were stored in sodium acetate buffer solution (0.1 M, pH 4.5) at 4 °C for a 30-day period. The free enzyme lost 82% its activity within 30 days, whereas the immobilized laccase lost only 35% of its initial activity over the same period (Figure 11A). This result indicates that the stability of immobilized laccase is highly improved compared to that of the free enzyme.[22] On the basis of this observation, modified hydrophilic support should provide a stabilization effect, minimizing possible distortion effects imposed by aqueous medium on the active site of the immobilized enzyme. Thus, the modified hydrophilic support and the immobilization method provide higher shelf life compared to that of its free counterpart. The result revealed that immobilized laccase has potential application in dyestuff treatment.[33]

The reusability of prepared immobilized enzymes is one of the most important aspects for industrial applications, because immobilization of enzymes decreases the cost of production due to their repeated continuous uses.[31,34,35] The repeated use experiments (Figure 11B) showed that the immobilized laccase on poly(MA-alt-MVE)g-PLA/ODA-MMT nanocomposite can be reused for 10 cycles for the degradation of Reactive Red 3.

The immobilized enzyme retained more than 75% of its initial activity after 10 consecutive repeated uses.[36] The activity loss in these steps may be related to the inactivation of enzyme upon use. The result showed that immobilized laccase has potential application in textile industry effluent treatment. Successful reuse of various immobilized laccase systems has been reported by other investigators.[37,38]
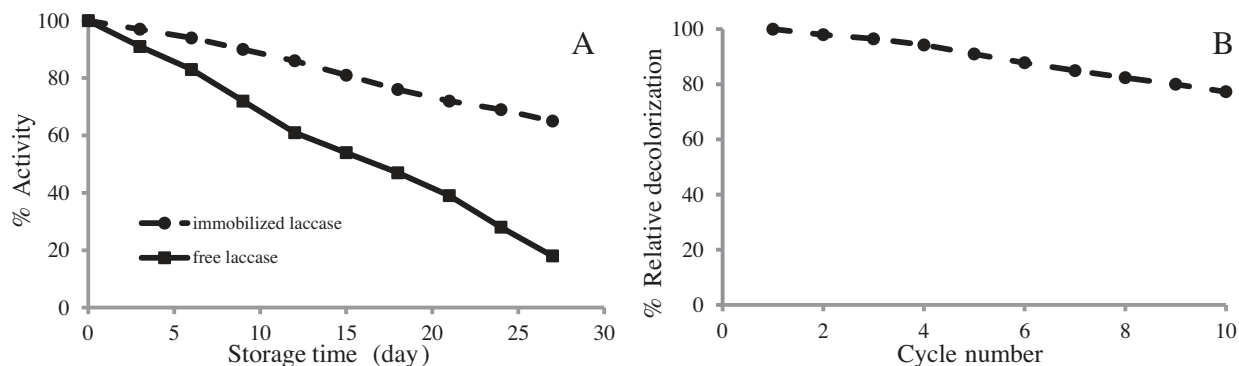
Figure 11. Storage stability (A) curves of immobilized and free laccase and activity of reuse (B) on decolorization of poly(MA-*alt*-MVE)-*g*-PLA/ODA-MMT immobilized enzyme.

3. Conclusions

We have developed a facile and effective strategy for the design of protein immobilized support. Unlike the known methods, where hazardous tin-containing catalyst is commonly used, the novel approach involves the use of pre-intercalated LA/ODA-MMT complex as catalyst-nanofiller (dual functionality) to prepare nanohybrid systems with intercalated/exfoliated graft copolymer/silicate layered nanoarchitectures that exhibit a finely dispersed surface and inner morphology. This strategy can also be broadly utilized in other anhydride-containing polymers such as random, alternating, and graft copolymers of MA with given hydrophilic/hydrophobic interaction balance to synthesize a new generation of copolymer-*g*-biopolymer/silicate nanomaterials for nanoengineering and nanomedicine applications. Another important aspect of this strategy is that it provides an alternative for future industrial application of the synthesized carboxyl/amide and PLA branched copolymer/organo-MMT hybrids with large contact areas and porous surface morphology and their laccase enzyme immobilized complexes for the treatment of effluents from the dye, printing, and textile industries, as well as for bioengineering and filtration applications.

The results of the comparative analysis of decolorization activity of pristine laccase and immobilized laccase indicate a remarkable improvement in decolorization efficiency in the presence of an intercalated polymer nanocomposites matrix. The observed relatively high activity and stability immobilized laccase onto functional copolymer-*g*-biopolymer/assay can be explained by (1) higher biocompatibility of polymer Poly(MA-*alt*-MVE), (2) surfactant properties of copolymer and octadecyl amine intercalant, (3) the formation of strong hydrogen bonding and a hydrophobic/hydrophilic interfacial interaction between polymer and laccase macromolecules after physical adsorption of enzyme onto the polymer matrix of nanocomposites, (4) the large surface area of intercalated silicate layers and their higher absorption and ion exchangeable capacity.

4. Experimental

4.1. Material and reagents

Poly(MA-*alt*-MVE) copolymers (M_n =80.000 Da) and poly L-lactic acid (PLA) (98% analytical standard), octadecyl amine (ODA)-montmorillonite (MMT) organoclay (Nanomer 1.30E, Nanocor Corporation) and 2,2'-azino-bis(3-ethylbenzothiazoline-6-sulfonic acid (ABTS) were purchased from Sigma-Aldrich (Steinheim, Germany). EDAC (N-(3-dimethylaminopropyl)-N'-ethylcarbodiimide hydrochloride) was obtained from Merck (Hohenbrunn, Germany).

Laccase was isolated from *Trametes (Coriolus) versicolor* ATTC (200801), which was obtained from Eskişehir Osmangazi University (ESOGU) Biotechnology Laboratory, using the method described by Çabuk et al.[39] The azo-dye Reactive Red 3 (RR3) was supplied by Sarar Textile Co., Turkey. All other solvents and reagents used in the present study were of analytical grade.

4.2. Preparation and characterization of poly(MA-*alt*-MVE)-*g*-PLA/ODA-MMT

Synthesis of the graft copolymer/ODA-MMT nanocomposite was carried out in a mixture of two different PLA solutions previously prepared in two parts: poly(MA-*alt*-MVE) copolymer in PLA (0.01 M) and organoclay powder particles (3 wt % of copolymer) in PLA by intensive dispersing for 3 h until the homogeneous medium is obtained. The reaction media were blended for 3 h using a mixer where they were intensively mixed in a carousel type of micro-reactor at 80 °C up to the formation of a completely homogeneous viscose solution. Then the nanohybrid structure was precipitated with methanol (80 wt %) and washed three times with deionized water using centrifugation (9000 rpm, 15 min) and dried under a vacuum at 40 °C.

The Fourier transfer infrared (FT-IR) spectra were obtained with a FT-IR Nicolet 510 spectrometer by the standard KBr disk method in the range of 4000–500 cm^{-1} with a resolution of 4 cm^{-1}. ^{1}H $\{^{13}$C$\}$ NMR spectra were obtained on a JEOL 6X-400 (400 MHz) spectrometer with DMSO-d_6 as solvent at 25 °C.

The X-ray powder diffraction (XRD) patterns were recorded on a PANANALYTICAL X-ray diffractometer equipped with a CuK$_\alpha$ tube and Ni filter (λ = 1.5406 Å). The XRD diffractograms were measured at 2θ, in the range 1–50°. The Bragg equation was used to calculate the interlayer spacing (d): $n\lambda = 2d\sin\theta$, where n is the order of reflection and θ is the angle of reflection.

The surface morphology of the nanocomposite was examined using a ZEISS SUPRA 40 field emission scanning electron microscope (FESEM). The inner morphology of the nanocomposites was investigated by FEI Tecnai G^2 Spirit Biotwin model high contrast transmission electron microscopy (CTEM) with a Lantan Hexaboron Electron Gun at 120 kV.

The UV/vis absorption spectra were measured using a Shimadzu UV-1240 spectrophotometer.

4.3. Enzyme immobilization studies

Laccase was immobilized onto the poly(MA-*alt*-MVE)-*g*-PLA/ODA-MMT nanocomposite either by adsorption or by covalent binding on activated nanocomposite.

In the physical adsorption procedure 2.5 mg of the poly(MA-*alt*-MVE)-*g*-PLA/ODA-MMT nanocomposite was dispersed in 4 mL of sodium acetate buffer (0.1 M, pH 4.5) containing a certain amount of laccase (0.25 mg/mL). The mixture (nanocomposite and laccase) was stirred at room temperature for 6 h. Then laccase immobilized on the nanocomposite was separated by centrifugation and washed with buffer solution (10 mL) four times.

In the covalent coupling procedure 2.5 mg of the poly(MA-*alt*-MVE)-*g*-PLA/ODA-MMT nanocomposite was dispersed in 4 mL of sodium acetate buffer (0.1 M, pH 4.5) containing EDAC solution (0.5 mL, 2.5% w/v). The mixture was stirred at room temperature for 6 h. After that, nanocomposite activated by EDAC was separated by centrifugation and washed with buffer solution (10 mL) three times. Finally, the resulting support was used for immobilization of laccase under the same conditions as the first procedure.

A laccase immobilization assay was carried out in a concentration range between 0.01 and 0.15 mg/mL, the reaction time range 0–120 min in the reaction medium, over the pH range 3.5–7.5 (in 0.1 M acetate buffer, pH 3.5–5.5; in 0.1 M phosphate buffer, pH 6.0–7.4), and temperature range 4–60 °C for the determination of the effect of different conditions on immobilization.

The amount of bound protein was determined by Bradford's (BioRad protein assay) method,[40] using the following equation: $Q = (C_i - C_f)/mV$, where Q is the bound enzyme (mg enzyme/g nanocomposite), C_i and C_f are the initial and final enzyme concentrations in the solution (mg/mL), V is the volume of the solution (mL), and m is the mass of the nanocomposite (g).

Laccase activity was measured as the oxidation of ABTS by applying the method described by Çorman et al.[41] ABTS was chosen as substrate since laccases in general have high affinity for ABTS, which is oxidized to a stable green colored cationic radical, $ABTS^+$.[42,43] The reaction solution was composed of 1 mL of ABTS (0.5 mM) in 0.1 M sodium acetate buffer (pH 4.5) in a disposable cuvette. First 1 mL of purified enzyme solution or 0.25 mg of immobilized enzyme was added to the ABTS solution and incubated at 25 °C and 120 rpm for 30 min. As the control was used 1 mL of ABTS solution (0.5 mM) in 0.1 M sodium acetate buffer without enzyme. Change in absorbance at 420 nm was monitored by a UV/vis spectrophotometer and a calibration curve was plotted to calculate enzyme activity. The laccase activity was then calculated using the molar extinction coefficient of ABTS ($\varepsilon_{420} = 36,000\,M^{-1}\,cm^{-1}$). Activity in one unit (U) of laccase corresponds to the oxidation of 1 μmol ABTS/min under the assay conditions.[44] All experiments were performed in triplicate.

Enzyme immobilization yield and efficiency were determined indirectly by calculating the amounts of total bound enzyme on the nanocomposite using Bradford's total protein assay and measuring the activity of the immobilized enzyme per nanocomposite unit weight, respectively.

4.4. Degradation studies of textile dyes; optimum temperature, pH, dye concentration, and reaction time of the immobilized laccase

The effect of pH on enzymatic decolorization was calculated with a free and immobilized enzyme (0.25 mg/mL) at a 1–7.5 pH range adjusted by citrate (0.1 M) or phosphate buffers (0.1 M). The reaction mixture (a free and immobilized enzyme concentration of 0.25 mg/mL) was incubated at a thermal range of 4–60 °C to obtain the effect of temperature on enzymatic decolorization. In order to estimate the effect of dye quantity on decolorization, the reaction containing a free and immobilized enzyme (0.25 mg/mL) was started with different dye concentration values varying between 0.01 to 0.1 mg/L. To study the effect of reaction time on enzymatic decolorization, the reaction was conducted at a time range between 5 and 240 min. The experiments were performed in triplicate. Relative decolorization was calculated by the following equation:

$$\text{Relative decolorization (\%)} = (A_{initial} - A_{final})/A_{initial} \times 100,$$

where $A_{initial}$ is the initial absorbance and A_{final} is the final absorbance at the given wavelength.

4.5. Storage stability and reusability

Storage stability experiments were conducted to assess the stabilities of free and on support immobilized laccase on decolorization of Reactive Red 3 after storage in acetate buffer (0.1 M, pH 5.0) for 8 weeks. The reusability of immobilized laccase was determined with the decolorization of azo dye with a 90-min cycle run for 10 cycles. At the end of each cycle, immobilized laccase was separated from the nanocomposite and washed three times with acetate buffer solution (0.1 M, pH 5.0), and then a second cycle was performed. The activity of storage stability and reusability were then calculated as described above. The experiments were performed in triplicate.

Acknowledgment

References

1. Vandevivere, P.; Bianchi, R.; Verstraete, W. *J. Chem. Technol. Biotechnol.* **1998**, *72*, 289-302.

2. Beyene, H. D. *Int. J. Environ. Monit. Anal.* **2014**, *2*, 347-353.

3. Khouni, I.; Benoît, M.; Moulin, P.; Amar, R. B. *Desalination* **2011**, *268*, 27-37.

4. Jin, X; Ning, Y. *J. Hazard. Mater.* **2013,** *26*2, 870-877.

5. Jeon, J. R.; Baldrian, P.; Murugesan, K.; Chang, Y. S. *Micro. Biotech.* **2012**, *5*, 318-332.

6. Russo, M. E.; Giardina, P.; Marzocchella, A.; Salatino, P.; Sannia, G.; *Enzyme. Microb. Technol.* **2008**, *42*, 521-530.

7. Fernández-Fernández, M.; Sanromán, M. Á.; Moldes, D. *Biotechnol. Adv.* **2013**, *31*, 1808-1825.

8. Datta, S.; Christena, L. R.; Rajaram, Y. R. S. *3 Biotech.* **2013**, *3*, 1-9.

9. Yong, Y.; Bai, Y.; Li, Y.; Lin, L.; Cui, Y.; Xia, C. *J. Magn. Magn. Mater.* **2008**, *320*, 2350-2355.

10. Kalkan, N. A.; Aksoy, S.; Aksoy, E. A.; Hasırcı, N. *J. Appl. Polymer. Sci.* **2012**, *123*, 707-716.

11. Allard, L.; Cheynet, V.; Oriol, L.; Gervasi, G.; Imbert-Laurenceau, E.; Mandrand, B.; Delair, T.; Mallet, F. *Bioconjug. Chem.* **2004**, *80*, 341-348.

12. Pompe, T.; Renner, R.; Grimmer, M.; Herold, N.; Wemer, C. *Macromol. Biosci.* **2005**, *5,* 890-895.

13. Klose, T.; Welzel, P. B.; Wemer, C. *Colloids Surf. B Biointerfaces* **2006**, *51*, 1-9.

14. Rzayev, Z. M. O. In *Advances in Polyolefin Nanocomposites*; Taylor & Francis Ltd. Publisher, CRC Press: New York, NY, USA, 2010, pp. 87-127.

15. Demircan, D.; Kibarer, G.; Rzayev, Z. M. O. *Polym. Bull.* **2013**, *70*, 3185-3200.

16. Song, W.; Liu, H.; Chen, F.; Zhang, J. *Polymer* **2012**, *53*, 2476-2484.

17. Chen, J.; Li, X.; Cui, W.; Xie, C.; Zou, J.; Zou, B. *Polymer* **2010**, *51*, 6268-6277.

18. Kontou, E.; Niaounakis, M.; Georgiopoulos, P. *J. Appl. Polym. Sci.* **2011**, *122*, 1519-1529.

19. Zhu, Y.; Kaskel, S.; Shi, J.; Wage T.; Pée, K. H. *Chem. Mater.* **2007**, *19*, 6408-6413.

20. Qiu, H.; Xu, C.; Huang, X.; Ding, Y.; Qu, Y.; Gao, P. *J. Phys. Chem. C* **2009**, *113*, 2521-2525.

21. Durán, N.; Rosa, M. A.; D'Annibale, A.; Gianfred, L. *Enzyme. Microb. Technol.* **2002**, *31*, 907-931.

22. Doğan, T.; Bayram, E.; Uzun L.; Şenel, S.; Denizli, A. *J. Appl. Polym. Sci.* **2015**, *132*.

23. Zhang, Y.; Rochefort, D. *Process Biochem.* **2011**, *46*, 993-1000.

24. Mogharabi, M.; Nassiri-Koopaei, N.; Bozorgi-Koushalshahi, M.; Nafissi-Varcheh, N.; Bagherzadeh, G.; Faramarzi, M. A. *Bioinorg. Chem. Appl.* **2012**, *2012*.

25. Inagaki, S.; Guan, S.; Fukushima, Y.; Ohsuna, T., Terasaki, O. *J. Am. Chem. Soc.* **1999**, *121*, 9611-9614.

26. Melde, B. J.; Holland, B. T.; Blanford, C. F.; Stein, A. *Chem. Mater.* **1999**, *11*, 3302-3308.

27. Arıca, M. Y.; Altıntaş, B.; Bayramoğlu, G. *Bioresource Technol.* **2009**, *100*, 665-669.

28. Morozova, O. V.; Shumakovich, G. P.; Gorbacheva, M. A.; Shleev, S. V.; Yaropolov, A. I. *Biochem. (Mosc.)* **2007**, *72*, 1136-1150.

29. Asadgol, Z.; Forootanfar, H.; Rezaei, S.; Mahvi, A. H.; Faramarzi, M. A. *J. Environ. Health Sci. Eng.* **2014**, *12*, 93.

30. Xu, R.; Zhou, Q.; Li, F.; Zhang, B. *J. Chem. Eng.* **2013**, *222*, 321-329.

31. Mirzadeh, S. S.; Khezri, S. M.; Rezaei, S.; Forootanfar, F.; Mahvi, A. H.; Faramarzi, M. A. *J. Environ. Health Sci. Eng.* **2014**, *12*, 6.

32. Bayramoğlu, G.; Arica, M. Y. *J. Hazard. Mater.* **2008**, *156*, 148-155.

33. Kunamneni, A.; Ghazi, I.; Camarero, S.; Ballesteros, A.; Plou, F. J.; Alcalde, M. *Process Biochem.* **2008**, *43*, 169-178.

34. Sadighi, A.; Faramarzi, M. A. *J Taiwan Inst. Chem. Eng.* **2013**, *44*, 156-162.

35. Faramarzi, M. A.; Sadighi, A. *Adv. Coll. Interface Sci.* **2013**, *189-190*, 1-20.

36. Salis, A.; Pisano, M.; Monduzzi, M.; Solinas, V.; Enrico Sanjust, E. *J. Mol. Catal. B.* **2009**, *58*, 175-180.

37. Davis, S.; Burns, R. G. *Appl. Microbiol. Biot.* **1992**, *37*, 474-479.

38. Shuttleworth, K. L.; Bollag, J. M. *Enzyme Microb. Tech.* **1986**, *8*, 171-178.

39. Gedikli, S.; Aytar, A.; Buruk, Y.; Apohan, E.; Çabuk, A.; Yeşilada, Ö.; Burnak, N. *Turk. J. Biochem.* **2014**, *39*, 298-306.

40. Bradford, M. M. *Anal. Biochem.* **1976**, *72*, 248-254.

41. Çorman, M. E.; Öztürk, N.; Bereli, N.; Akgöl, S.; Denizli, A. *J. Mol. Catal. B-Enzym.* **2010**, *63*, 102-107.

42. Faramarzi, M. A.; Forootanfar, H. *Colloids Surf. B.* **2011**, *87*, 23–27.

43. Aghaie-Khouzania, M.; Forootanfar, H.; Moshfegh, M.; Khoshayand, M. R.; Faramarzi, M. A. *Biochem. Eng. J.* **2012**, *60*, 9-15.

44. Alberts, J. F.; Gelderblom, W. C. A.; Botha, A.; Vanzyl, W. H. *Int. J. Food Microbiol.* **2009**, *135*, 47-52.